

## Development of an *a priori* computational approach for brain uptake of compounds in an insect model system



Werner J. Geldenhuys <sup>a,b,\*</sup>, Jeffrey R. Bloomquist <sup>c</sup>

<sup>a</sup> Department of Pharmaceutical Sciences, School of Pharmacy, West Virginia University, Morgantown, WV, USA

<sup>b</sup> Department of Neuroscience, School of Medicine, West Virginia University, Morgantown, WV, USA

<sup>c</sup> Emerging Pathogens Institute, Entomology and Nematology Department, University of Florida, Gainesville, FL, USA

### ARTICLE INFO

#### Keywords:

Blood-brain barrier  
Cheminformatics  
QSAR  
Data mining  
QSPR

### ABSTRACT

Delivery of compounds to the brain is critical for the development of effective treatment therapies of multiple central nervous system diseases. Recently a novel insect-based brain uptake model was published utilizing a locust brain *ex vivo* system. The goal of our study was to develop *a priori*, *in silico* cheminformatic models to describe brain uptake in this insect model, as well as evaluate the predictive ability. The machine learning program Orange® was used to evaluate several machine learning (ML) models on a published data set of 25 known drugs, with *in vitro* data generated by a single laboratory group to reduce inherent inter-laboratory variability. The ML models included in this study were linear regression (LR), support vector machines (SVM), k-nearest neighbor (kNN) and neural nets (NN). The quantitative structure–property relationship models were able to correlate experimental logC<sub>tot</sub> (concentration of compound in brain) and predicted brain uptake of  $r^2 > 0.5$ , with the descriptors log(P\*MW<sup>-0.5</sup>) and hydrogen bond donor used in LR, SVM and KNN, while log(P\*MW<sup>-0.5</sup>) and total polar surface area (TPSA) descriptors used in the NN models. Our results indicate that the locust insect model is amenable to data mining chemoinformatics and *in silico* model development in CNS drug discovery pipelines.

Drug delivery to the brain is a bottleneck for the development of therapies due to the presence of the blood–brain barrier (BBB).<sup>1</sup> The BBB is a microvascular unit which is comprised of vascular endothelial cells, pericytes, astrocytes and neuronal innervation.<sup>2</sup> Due to the presence of tight junctions between the endothelial cells, along with other processes such as efflux pumps (ABC cassette transporters including p-glycoprotein (PGP)), this selectively permeable system allows only certain compounds/xenobiotics with appropriate chemical properties to be able to distribute into the central nervous system (CNS) space, and contributes to a high failure rate in drug development of CNS drugs.<sup>1–3</sup>

Several techniques have been developed to determine uptake of compounds into the brain, including both *in vitro* and *in vivo* models.<sup>4</sup> Classical *in vitro* techniques include the use of other types of cells that express tight junctional proteins, including the kidney cell lines.<sup>5</sup> *In vivo* models include the determination of the log([Brain]/[Blood]) or logBB, where the drug is usually administered via an I.P. or tail vein I.V. injection and the brain removed usually after an hour to determine drug levels. Alternatively, a more technically advanced determination of the permeability–surface area product (PS) as measure of the passive drug

permeability across the BBB, after *in vivo* drug perfusion via cardiac or carotid artery delivery.<sup>6,7</sup> Due to the technical skill and analytical tools needed for their performance, these *in vivo* models can be a bottleneck in the compound characterization stage of the drug development pipeline.

Andersson *et al.* described a novel brain uptake model utilizing an *ex vivo* insect brain, isolated from desert locusts (*Schistocerca gregaria*).<sup>8</sup> The insect brain mimics the mammalian BBB with tight junctions found in perineurial glia protecting the brain.<sup>9</sup> An added benefit of using *ex vivo* insect brain is the lack of capillaries which could confound brain uptake determinations.<sup>8</sup>

Both *in vitro* and *in vivo* animal models have been used to develop predictive *in silico* models that can be applied to the early stages of drug discovery to filter compound databases, but to date no machine learning cheminformatic models have been developed for compound uptake in insect brain. These *in silico* quantitative structure–property relationship (QSPR) studies can be used in concert with these insect models on larger compound numbers, allowing for refinement in mammalian systems of lead compounds, depending on a company's specific workflow. The goal of this work was to utilize cheminformatic strategies to develop initial

\* Corresponding author at: 1 Medical Center Drive, Morgantown WV 26506, USA.

E-mail address: [werner.geldenhuys@hsc.wvu.edu](mailto:werner.geldenhuys@hsc.wvu.edu) (W.J. Geldenhuys).

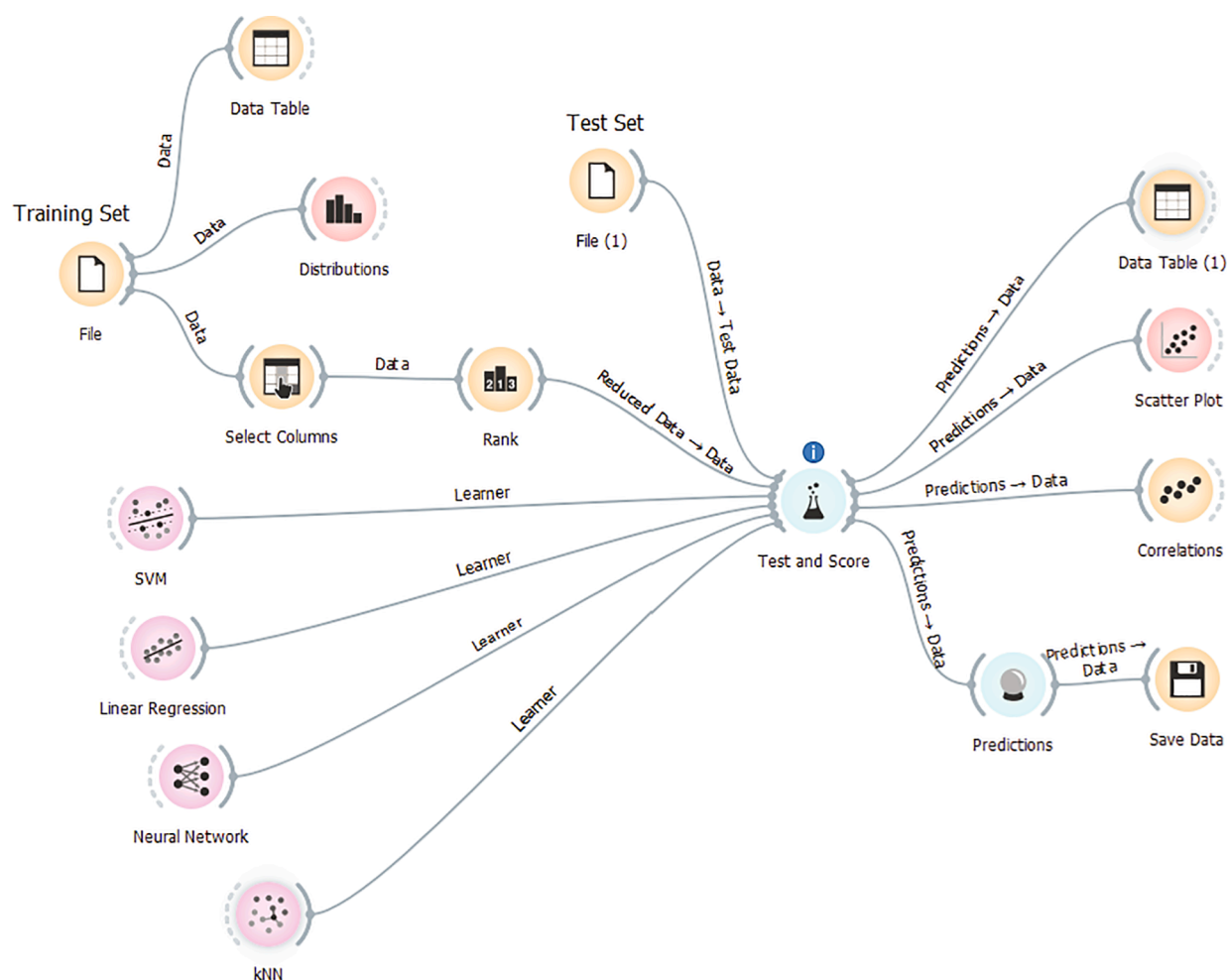


**Fig. 1.** Chemoinformatic workflow diagram utilized in Orange® data mining software version 3.24.1. Each widget is linked in a workflow for model development and testing. Abbreviations are: support vector machines (SVM); k-nearest neighbor (kNN).

data models that could be used *a priori* to screen compound libraries virtually and select a pool of candidates with higher propensity to reach the brain in CNS drug discovery programs.

We developed a database from compounds reported earlier with uptake into locust brain ( $N = 25$ ).<sup>8</sup> The chemical structures were obtained from PubChem as structure data file (SDF) files, combed into a single SDF, and imported into InstantJChem v. 16.8.15.0 ([www.chemaxon.com](http://www.chemaxon.com)). InstantJChem is a cheminformatics suite that can estimate physicochemical properties of each chemical compound. For the cheminformatics analysis, we utilized the machine learning (ML) software suite Orange® v 3.24. ([orange.biolab.si](http://orange.biolab.si)). Orange® is a widget-based system where workflows can be designed to suit specific ML needs of the user. Fig. 1 shows the workflow developed for this study.

The data sets obtained from the literature were reported from experiments where the drug exposures were a constant  $10 \mu\text{M}$  to the *ex vivo* insect brain, and was presented as  $C_{\text{tot}}$ , which we converted to  $\log C_{\text{tot}}$ , since this allows for smoothing of biological data. The  $\log C_{\text{tot}}$  value was used as the target ( $y$ ) variable in the Orange® software. We chose to use this value as described by Andersson *et al.*, due to the high degree of correlation between the *ex vivo* model of  $10 \mu\text{M}$  compound with mammalian permeability-surface values ( $\log PS$ ),<sup>10</sup> and the published  $r^2$  of 0.85 supported this dataset as correlative for mimicking mammalian brain uptake.<sup>8</sup> The physicochemical properties determined with InstantJChem were kept as features ( $x_n$ ).

Based on previous reports by Liu *et al.*, which described the development of computational approaches to brain uptake in mammals,<sup>11</sup> we additionally calculated the  $\log(D^*MW^{-0.5})$ , and  $\log(P^*MW^{-0.5})$

parameters. The database was split into a training set and a test set randomly, 72:28%, or 18 training and 7 test set compounds using the DATASAMPLER utility, and all compounds were considered inliers due to the small sample size. Although the initial dataset contained known p-glycoprotein (PGP) substrates,<sup>8</sup> we did not separate these into subsets, due to the small number of compounds in our set, as well as our goal of evaluating these for development of an *a priori* BBB *in silico* filter, i.e. used to screen libraries without prior knowledge of PGP transporter preference. Additionally, it is suggested that at the test concentration of compounds at  $10 \mu\text{M}$ , the PGP transporters may be saturated in the locust system, which could account for a passive permeability apparent state.<sup>8</sup>

Four ML systems were tested, including support vector machines (SVM), neural network (NN), k-nearest neighbor (kNN) and multiple linear regression (LR). To identify and rank important descriptors, the RANK utility with the regression correlation value ( $r$ ) was used, which identified  $\text{clogP}$  (where  $P$  is ratio octanol/water separation),  $\text{clogD}$  ( $\log D$  at a pH of 7.4),  $\log(D^*MW^{-0.5})$ , and  $\log(P^*MW^{-0.5})$ , hydrogen bond donors, total polar surface area (TPSA) as the top parameters. With only 18 compounds in the training set, we set our upper limit to the number of variables to  $\leq 4$  descriptors, to prevent overfitting of the data.<sup>12,13</sup> We opted to focus on the minimum number of descriptors, after which no discernable improvement could be seen in the training set regression value ( $r^2$ ), when additional descriptors were added. Additionally, due to the relationship between  $\text{clogP}$  and  $\text{clogD}$  where  $\text{clogD} = \text{clogP} + p\text{Ka}$  at pH 7.4, we opted to not combine these two parameters in a single model, due to a duplication of properties. Table 1 shows the training data set

**Table 1**  
Training set used to develop the ML models.

Drug	logCtot*	clsgD	Mol Weight	TPSA	H bond acceptors	H bond donors	Ring count	clsgP	Rotatable Bonds	Bioavailability	logMW <sup>-0.5</sup>	Log(P*MW <sup>-0.5</sup> )	Log(D*MW <sup>-0.5</sup> )
desipramine	1.0414	1.37	266.39	15.27	2	1	3	3.9	4	TRUE	-1.21276	2.68	0.16
dexamethasone	0.0000	1.68	392.47	94.83	5	3	4	1.68	2	TRUE	-1.2969	0.38	0.38
haloperidol	0.9868	2.39	239.74	29.1	2	1	1	3.27	4	TRUE	-1.18987	2.08	1.2
cyclosporin A	0.415	3.64	1202.64	278.8	12	5	1	3.64	15	FALSE	-1.54007	2.1	2.1
loperamide	0.7924	2.77	477.05	43.78	3	1	4	4.77	7	TRUE	-1.33928	3.43	1.43
fluoxetine	1.2967	1.83	309.33	21.26	2	1	2	4.17	7	TRUE	-1.24521	2.93	0.58
propranolol	0.9085	0.36	259.35	41.49	3	2	2	2.58	6	TRUE	-1.20694	1.38	-0.85
amitriptyline	1.1761	2.48	277.41	3.24	1	0	3	4.81	3	TRUE	-1.22156	3.59	1.26
ranitidine	-0.699	0.45	314.4	83.58	5	2	1	0.99	10	TRUE	-1.24874	-0.26	-0.8
cetirizine	0.3424	0.65	388.89	53.01	5	1	3	0.87	8	TRUE	-1.29491	-0.42	-0.64
atenolol	-0.699	-1.8	266.34	84.58	4	3	1	0.43	8	TRUE	-1.21272	-0.79	-3.01
norfloxacin	-0.0969	-0.92	319.34	72.88	6	2	3	-0.92	3	TRUE	-1.25212	-2.17	-2.17
trazodone	0.9638	2.96	371.87	42.39	4	0	4	3.13	5	TRUE	-1.2852	1.85	1.67
caffeine	0.7404	-0.55	194.19	58.44	3	0	2	-0.55	0	TRUE	-1.14412	-1.69	-1.69
carbamazepine	1.2041	2.77	236.27	46.33	1	1	3	2.77	0	TRUE	-1.18671	1.58	1.58
digoxin	-0.0969	1.92	780.95	203.06	13	6	8	2.37	7	FALSE	-1.44631	0.92	0.48
paroxetine	1.3979	0.83	329.37	39.72	4	1	4	3.15	4	TRUE	-1.25884	1.89	-0.43
lincomycin	-0.5229	-0.99	406.54	122.49	7	5	2	-0.32	7	TRUE	-1.30455	-1.62	-2.29

\*Experimental concentration of compound in locust brain

**Table 2**  
Test set for validation of ML models.

Drug	logCtot*	logD	Mol Weight	TPSA	H bond acceptors	H bond donors	Ring count	logP	Rotatable Bonds	Bioavailability	logMW <sup>-0.5</sup>	Log(P*MW <sup>-0.5</sup> )	Log(D*MW <sup>-0.5</sup> )
methotrexate	-0.699	-6.56	454.45	210.54	12	5	3	-0.24	9	FALSE	-1.32874	-1.57	-7.89
warfarin	0.6721	0.94	308.33	63.6	3	1	3	2.74	4	TRUE	-1.24451	1.5	-0.3
citalopram	0.6628	1.41	324.4	36.26	3	0	3	3.76	5	TRUE	-1.25554	2.5	0.15
haloperidol	1.1271	2.93	375.87	40.54	3	1	3	3.66	6	TRUE	-1.28752	2.37	1.64
risperidone	0.9138	1.25	410.49	61.94	4	0	5	2.63	4	TRUE	-1.30665	1.32	-0.06
quinidine	0.5051	0.86	324.42	45.59	4	1	4	2.51	4	TRUE	-1.25556	1.26	-0.39
cimetidine	-0.3979	-0.22	252.34	88.89	5	3	1	-0.11	5	TRUE	-1.20099	-1.31	-1.42

\*Experimental concentration of compound in locust brain

**Table 3**Cross-validation ( $q^2$ ) of machine learning models.

Cross-validated regression ( $q^2$ )	Log ( $P^*MW^{-0.5}$ )	logP	logDMW	HB DONOR	logD	TPSA	Log ( $P^*MW^{-0.5}$ )	Log ( $P^*MW^{-0.5}$ )	logP	logP
KNN	0.5	0.476	-0.024	0.423	-0.052	0.688	0.718	HB DONOR	0.666	0.725
SVM	0.354	0.326	0.233	0.178	0.149	-0.636	0.639	0.549	0.62	0.549
NN	0.429	0.386	0.185	0.41	0.153	0.686	0.688	0.704	0.68	0.689
LR	0.39	0.347	0.237	0.286	0.177	-0.38	0.622	0.475	0.618	0.467

with the calculated parameters, and **Table 2** shows the training set data.

A main advantage of using Orange® ML, is that several machine learner algorithms can be tested at the same time (see **Fig. 1**). Using 10-fold cross-validation, we used the training set of 18 compounds to develop the models, with results of the cross-validation regression value ( $q^2$ ) shown in **Table 3**. The method of cross-validation generates a model on the training set, and removes one compound at a time, and predicts that compound's biological parameter being investigated, which in this case is  $\log C_{tot}$ . The cross validated  $q^2$  values  $> 0.3$  were generally regarded as significant for quantitative structure–activity relationship (QSAR) models,<sup>14,15</sup> although recent literature suggests that  $q^2 > 0.5$  be considered a more significant cut-off value to evaluate the robustness of a computational QSPR models.<sup>12,13</sup>

Based on this last literature criterion, for a single variable correlating experimental brain uptake ( $\log C_{tot}$ ) with molecular descriptors, the TPSA resulted in  $q^2$  values  $> 0.5$ , for only the KNN and NN models, while SVN and LR showed negative or no correlation. This result led us to include a combination of at least two descriptors to improve model development. We found that the combination of  $\log(P^*MW^{-0.5})$  with HB DONOR or TPSA, and logP with HB DONOR and TPSA led to favorable  $q^2 > 0.5$  ML models (**Table 3**). Interestingly, the use of logD did not lead to any improved model outcomes, as has been shown with mammalian *in silico* filters,<sup>10</sup> and in most cases impacted the model development negatively, i.e. reduced the cross validated  $q^2$  score. The observation that logD does not improve the QSPR models could possibly be linked to differences between this insect model versus mammalian systems. In insects, the glia forms the tight junctions and there is a lack of circulatory micro-vessels, corroborating the observation that logP (lipophilicity) may be more important than logD (lipophilicity at pH 7.4). For the purpose of modeling BBB permeability, these findings would suggest that possible use of a logP-based predictive model to be more beneficial when an insect/locust *in vivo* model will be used as lower level screening validation, while a logD-based filter more suited when a mammalian models will be used downstream.

To further validate the performance of the models, we used the prepared test set of seven compounds and used the developed ML models to predict brain uptake (predicted  $\log C_{tot}$ ). **Fig. 2** shows the correlation plots of the results from the (A) training set correlations; (B) test set correlations, as well as the residual plots of the (C) training set predictions and (D) test set predictions. **Table 4** shows the resulting correlation linear regression  $r^2$  for each of the models, and **Tables 5** and **6** show the predicted values for brain uptake generated by the different ML models. Interestingly, for the training set, the NN showed the highest correlation, with an  $r^2$  of 0.9, but performed worse on the test set, with an  $r^2$  of 0.8 as compared to the rest of the models. This difference is likely due to the small number of compounds used in this study and at the time that additional data sets become available in the literature, refinement of the current data models will be possible.

Andersson *et al.* showed that the grasshopper brain model can be used as an *ex vivo* platform in identifying BBB permeable compounds in

mammals.<sup>8</sup> As part of the validation process, the group correlated the logCtot from the locust model with the Permeability-Surface area (PS) parameter previously published in a mammalian system.<sup>10</sup> The logPS method uses an *in situ* perfusion method, correlating permeability as linear uptake over a min, and although intensive, is considered a true representative parameter for BBB permeability, in contrast to logBB ([brain]/[plasma]) which is in general determined at a 30 min or 1 h timepoint.<sup>16</sup> To explore the use of the ML models in predicting or classifying compounds as BBB permeable in mammals, the correlation of logPS in mice with the logCtot in locust was repeated from the published study, and we found to corroborate the published finding of  $r^2$  of 0.87 (**Fig. 3**; **Table 7**). Extending this correlation to the predicted logCtot values from **Table 5**, we found all of the ML models predicted logCtot were correlating well with logPS, with regression coefficients of 0.86 (SVN), 0.86 (LR), 0.82 (NN) and 0.84 (kNN). These findings support the use of computational models together with insect *ex vivo* brain models to augment discovery pipelines as possible pre-murine/rat seeing toolset.<sup>8,10</sup>

A limitation of the current study is the size of the insect data set published.<sup>8</sup> To gain some insight into the use of the models in clustering compounds into a mammalian BBB permeable (BBB+), versus excluded (BBB-), we evaluated the performance of these insect ML models on classifying an external dataset of compounds consisting of 479 BBB- and 1429 BBB+ compounds. We labeled the external test compounds for the classification as BBB+ and BBB-, which for our evaluation, was BBB+ as  $\log BB > 0$ , and BBB- as  $\log BB < 0$ , keeping with the convention of the published set.<sup>17</sup> We found that for the BBB- compounds in the external set, the kNN model performed the best, with correctly classifying 78% of the BBB- compounds, while the other ML models performed poorer, with NN 45%, LR 40% and SVN 37% successful classification as BBB- compounds. The ML models performed on average better on classifying BBB+ compounds, with kNN 68%, NN 89%, LR 93% and SVN 93% correct classification of BBB+ compounds.

Furthermore, the ML models were used to predict locust brain uptake of clozapine, a CNS therapeutic which was not included in the original locust dataset (Tab. 1 and 2) but was recently evaluated by the group of Hellman *et al.* in locust *ex vivo* model,<sup>18</sup> with our predicted ML model logCtot to range between 0.8 and 1.1. The logPS of clozapine is -1.73 mL/g/s in mice,<sup>10</sup> thus corroborating the insect locust model use for evaluating BBB permeability as part of a drug discovery pipeline towards mammalian systems. Taken together, the insect ML models will likely require additional parameterization as larger datasets become available for effective mammalian BBB permeability prediction, since these models performed well at classifying BBB permeable compounds, but fared worse at identifying compounds likely to be excluded from the BBB. Additionally, since PGP substrates were included in our ML model training, further dividing the training datasets would likely improve the predictive and classifier aspects of the models.<sup>18</sup>

In conclusion, we used cheminformatic-based machine learning to develop models for a small set of compounds for brain uptake in an *ex*

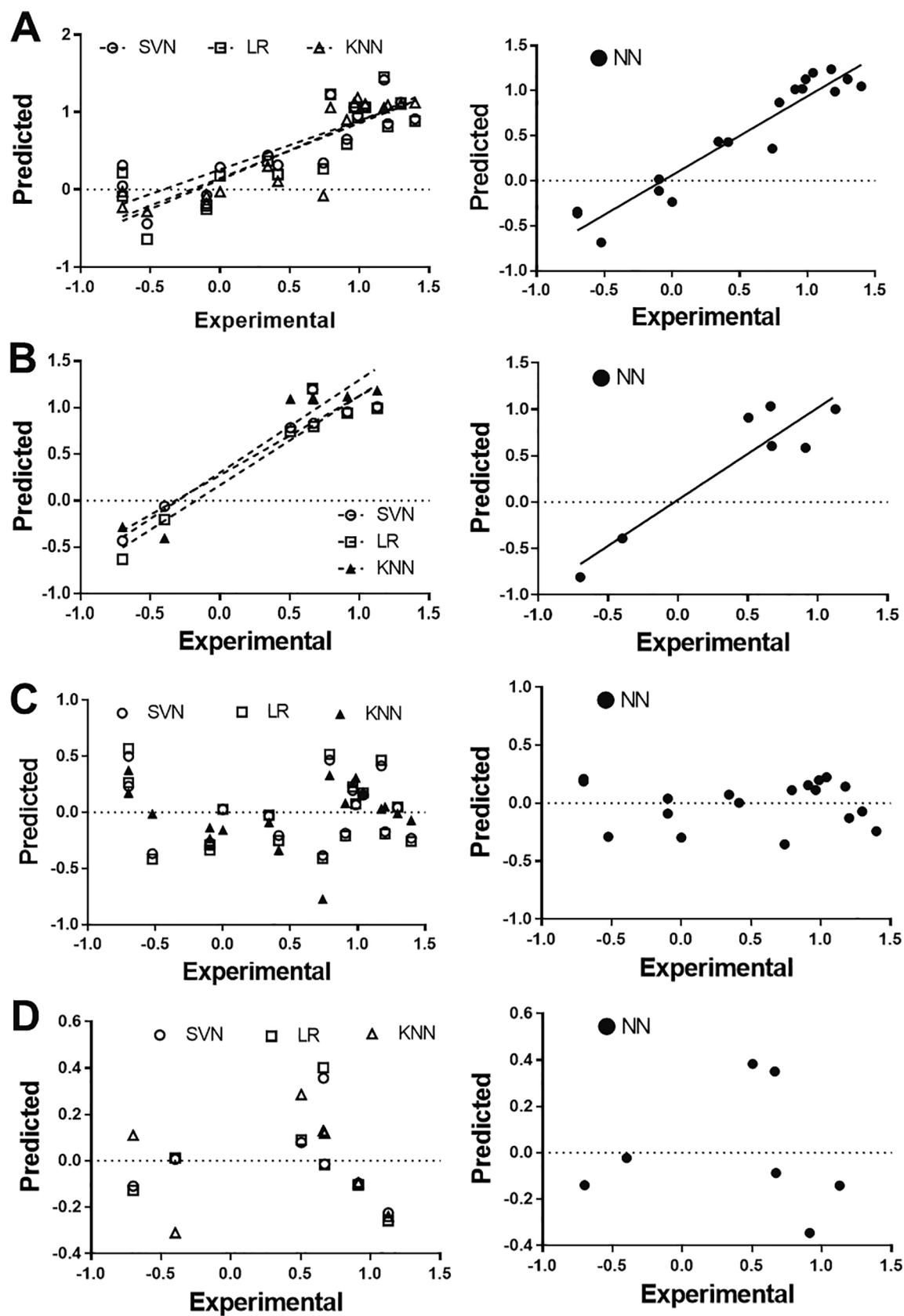


**Fig. 2.** Results from the ML training and test set correlation experimental brain uptake ( $\log C_{\text{tot}}$ ) with predicted values. Results from the A) training set correlation, B) test set correlation, C) residual plots of the training, and D) residual plots of the test sets, for the SVN, LR, KNN and NN models.

**Table 4**

Results from the ML training and test set correlating experimental brain uptake ( $\log C_{tot}$ ) with predicted values.

Training Set	SVN	LR	KNN	NN
$r^2$	0.7122	0.7124	0.7871	0.9109
Equation	$Y = 0.6333 \cdot X + 0.2565$	$Y = 0.7124 \cdot X + 0.1462$	$Y = 0.7598 \cdot X + 0.1259$	$Y = 0.8775 \cdot X + 0.06194$
Test Set	SVN	LR	KNN	NN
$r^2$	0.9078	0.9072	0.9058	0.8624
Equation	$Y = 0.8520 \cdot X + 0.2737$	$Y = 0.9602 \cdot X + 0.1673$	$Y = 0.9961 \cdot X + 0.3031$	$Y = 0.9919 \cdot X + 0.02604$

**Table 5**

Predicted brain uptake values ( $\log C_{tot}$ ) for the training set of compounds for each of the ML models.

Descriptors used in model development	Log( $P^*MW^{-0.5}$ )HBOND			
	$\log C_{tot}$	SVN	LR	KNN
Drug	Experimental	Predicted		
desipramine	1.041	1.073	1.061	1.103
dexamethasone	0.000	0.285	0.176	-0.029
bupropion	0.987	0.951	0.927	1.185
cyclosporin A	0.415	0.316	0.193	0.106
loperamide	0.792	1.225	1.230	1.059
fluoxetine	1.297	1.123	1.118	1.103
propranolol	0.909	0.648	0.585	0.899
amitriptyline	1.176	1.417	1.450	1.054
ranitidine	-0.699	0.315	0.217	-0.029
cetirizine	0.342	0.442	0.366	0.298
atenolol	-0.699	0.047	-0.086	-0.231
norfloxacin	-0.097	-0.074	-0.212	-0.082
trazodone	0.964	1.064	1.060	1.119
caffeine	0.740	0.344	0.265	-0.082
carbamazepine	1.204	0.849	0.815	1.092
digoxin	-0.097	-0.084	-0.256	-0.181
paroxetine	1.398	0.912	0.884	1.119
lincomycin	-0.523	-0.441	-0.642	-0.283
				-0.685

**Table 6**

Results from the ML test set correlating experimental brain uptake ( $\log C_{tot}$ ) with predicted values.

Descriptors used in model development	Log( $P^*MW^{-0.5}$ )HBOND			
	$\log C_{tot}$	SVN	LR	KNN
Drug	Experimental	Predicted		
methotrexate	-0.699	-0.431	-0.631	-0.283
warfarin	0.672	0.833	0.797	1.092
citalopram	0.663	1.196	1.206	1.093
haloperidol	1.127	1.010	0.992	1.185
risperidone	0.914	0.956	0.941	1.119
quinidine	0.505	0.784	0.743	1.092
cimetidine	-0.398	-0.058	-0.203	-0.404
				-0.390

*ex vivo* insect model. These *in silico* database filtering models can support virtual screening in drug discovery for CNS diseases, including Alzheimer's disease, Parkinson's disease, stroke and brain-associated cancers. The gap in our study is the size of the published data set, for which improvement of the current models will occur when larger datasets in the locust model become available for additional data modeling and gaining further insight into correlating locust BBB *ex vivo* models with mammalian BBB models.

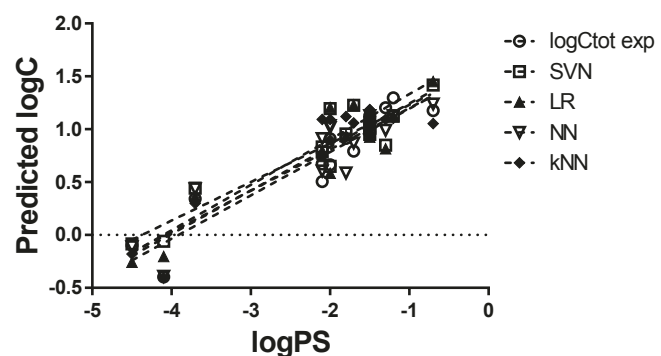


**Fig. 3.** Correlation of the Permeability-surface area (PS) in mammal as measure of brain uptake with locust  $\log C_{tot}$ . The ML model prediction of  $\log C_{tot}$  was correlated to  $\log PS$  as described.  $\log C_{tot}$  experimental is also shown as benchmark. The regression coefficient ( $r^2$ ) for the different ML models were  $> 0.8$ ,

**Table 7**

Permeability-Surface Area ( $\log PS$ ) of compounds from mammalian studies.<sup>8,10</sup>

Compound	$\log C_{tot}$	$\log PS$ (mL/g/min)
amitriptyline	1.18	-0.66
bupropion	0.99	-1.52
carbamazepine	1.20	-1.26
cetirizine	0.34	-3.72
cimetidine	-0.40	-4.1
citalopram	0.66	-1.99
digoxin	-0.10	-4.55
fluoxetine	1.30	-1.2
haloperidol	1.13	-1.46
loperamide	0.79	-1.7
propranolol	0.91	-2.15
quinidine	0.51	-2.11
risperidone	0.91	-1.8
trazodone	0.96	-1.5
warfarin	0.67	-2.1

## Declaration of Competing Interest

The authors declare that they have no known competing financial interests or personal relationships that could have appeared to influence the work reported in this paper.

## Acknowledgments

This material is based upon work supported by the National Science Foundation I/UCRC, the Center for Arthropod Management Technologies under Grant No. IIP-1821914 and by industry partners. The project described was supported by the National Institute Of General Medical Sciences, U54GM104942 and P20 GM109098. The content is solely the responsibility of the authors and does not necessarily represent the official views of the NIH. The graphical abstract was in part created with vector-based illustrations (grasshopper, neural network, mouse brain) from BioRender.com.

## References

- 1 Pardridge WM. Blood-brain barrier delivery. *Drug Discov Today*. 2007;12(1-2):54–61. <https://doi.org/10.1016/j.drudis.2006.10.013>.

2 Abbott NJ, Patabendige AAK, Dolman DEM, Yusof SR, Begley DJ. Structure and function of the blood-brain barrier. *Neurobiol Dis.* 2010;37(1):13–25. <https://doi.org/10.1016/j.nbd.2009.07.030>.

3 Geldenhuys WJ, Mohammad AS, Adkins CE, Lockman PR. Molecular determinants of blood-brain barrier permeation. *Ther Deliv.* 2015;6(8):961–971. <https://doi.org/10.4155/td.15.32>.

4 Bickel U. How to measure drug transport across the blood-brain barrier. *NeuroRx.* 2005;2(1):15–26. <https://doi.org/10.1602/neurrx.2.1.15>.

5 Veszelka S, Tóth A, Walter FR, et al. Comparison of a Rat Primary Cell-Based Blood-Brain Barrier Model With Epithelial and Brain Endothelial Cell Lines: Gene Expression and Drug Transport. *Front Mol Neurosci.* 2018;11. <https://doi.org/10.3389/fnmol.2018.0016610.3389/fnmol.2018.00166.s001>.

6 Smith QR. In: *Blood-Brain Barrier*, New Jersey: Humana Press; 2003:193–208. <https://doi.org/10.1385/1-59259-419-0.193>.

7 Smith QR, Allen DD. In situ brain perfusion technique. *Methods Mol Med.* 2003;89: 209–218. <https://doi.org/10.1385/1-59259-419-0:209>.

8 Andersson O, Hansen SH, Hellman K, et al. The grasshopper: a novel model for assessing vertebrate brain uptake. *J Pharmacol Exp Ther.* 2013;346(2):211–218. <https://doi.org/10.1124/jpet.113.205476>.

9 Geldenhuys WJ, Allen DD, Bloomquist JR. Novel models for assessing blood-brain barrier drug permeation. *Expert Opin Drug Metab Toxicol.* 2012;8(6):647–653. <https://doi.org/10.1517/17425255.2012.677433>.

10 Dagenais C, Avdeef A, Tsimman O, Dudley A, Beliveau R. P-glycoprotein deficient mouse in situ blood-brain barrier permeability and its prediction using an in combo PAMPA model. *Eur J Pharm Sci.* 2009;38(2):121–137. <https://doi.org/10.1016/j.ejps.2009.06.009>.

11 Liu X, Tu M, Kelly RS, Chen C, Smith BJ. Development of a computational approach to predict blood-brain barrier permeability. *Drug Metab Dispos.* 2004;32(1):132–139. <https://doi.org/10.1124/dmd.32.1.132>.

12 Alexander DLJ, Tropsha A, Winkler DA. Beware of R(2): Simple, Unambiguous Assessment of the Prediction Accuracy of QSAR and QSPR Models. *J Chem Inf Model.* 2015;55(7):1316–1322. <https://doi.org/10.1021/acs.jcim.5b00206>.

13 Golbraikh A, Tropsha A. Beware of  $q^2$ . *J Mol Graph Model.* 2002;20(4):269–276. [https://doi.org/10.1016/S1093-3263\(01\)00123-1](https://doi.org/10.1016/S1093-3263(01)00123-1).

14 Geldenhuys WJ, Allen DD, Lockman PR. 3-D-QSAR and docking studies on the neuronal choline transporter. *Bioorg Med Chem Lett.* 2010;20(16):4870–4877. <https://doi.org/10.1016/j.bmcl.2010.06.090>.

15 Geldenhuys WJ, Manda VK, Mittapalli RK, et al. Predictive screening model for potential vector-mediated transport of cationic substrates at the blood-brain barrier choline transporter. *Bioorg Med Chem Lett.* 2010;20(3):870–877. <https://doi.org/10.1016/j.bmcl.2009.12.079>.

16 Geldenhuys WJ, Lockman PR, Philip AE, et al. Inhibition of choline uptake by N-cyclohexylcholine, a high affinity ligand for the choline transporter at the blood-brain barrier. *J Drug Target.* 2005;13(4):259–266. <https://doi.org/10.1080/10611860500139222>.

17 Kortagere S, Chekmarev D, Welsh WJ, Ekins S. New predictive models for blood-brain barrier permeability of drug-like molecules. *Pharm Res.* 2008;25(8): 1836–1845. <https://doi.org/10.1007/s11095-008-9584-5>.

18 Hellman K, Aadal Nielsen P, Ek F, Olsson R. An ex Vivo Model for Evaluating Blood-Brain Barrier Permeability. *Efflux, and Drug Metabolism. ACS Chem Neurosci.* 2016;7 (5):668–680. <https://doi.org/10.1021/acschemneuro.6b0002410.1021/> [acschemneuro.6b00024.s001](https://doi.org/10.1021/acschemneuro.6b00024.s001).